

**Reference-free cable damage detection using magnetostrictive  
transducer-based guide wave method**

Xiao-dong Sui<sup>1)</sup>, \*Chung-bang Yun<sup>2)</sup>, Yuan-feng Duan<sup>3)</sup> and Zhi-feng Tang<sup>4)</sup>

<sup>1),2),3)</sup> *College of Civil Engineering and Architecture, Zhejiang University, China*

<sup>4)</sup> *Institute of Advanced Digital Technologies and Instrumentation, Zhejiang University,  
China*

<sup>1)</sup> [11712067@zju.edu.cn](mailto:11712067@zju.edu.cn)

<sup>2)</sup> [ycb@zju.edu.cn](mailto:ycb@zju.edu.cn)

<sup>3)</sup> [ceyfduan@zju.edu.cn](mailto:ceyfduan@zju.edu.cn)

<sup>4)</sup> [tangzhifeng@zju.edu.cn](mailto:tangzhifeng@zju.edu.cn)

**ABSTRACT**

A magnetostrictive (MS) transducer-based guided wave method is presented for cable damage detection in this study. A reference-free method is proposed to estimate the damage severity based on the reduction of the wave energy transmission coefficient at damage location. Firstly, the semi-analytical finite element (SAFE) method is employed on a steel strand with 7 wires for analyzing the wave dispersion properties including the wave modes, excitation frequencies, and corresponding wave velocities. Then, a MS transducer is designed to generate and receive the guided waves, which consists of a permanent magnet unit and a coil unit. Numerical and experimental studies are carried on the steel strand with various cases of wire breakage and corrosion using the pulse-echo method. The Hilbert transform is applied on the reflected wave packets of the measured signals to obtain their time of flight information, which is used for damage localization. Besides, the wavelet coefficients at the excitation frequency are used to calculate the transmitted and reflected wave energy for the wave packets reflected from the damage. It has been found that the damage locations and severities can be determined very effectively using the proposed method.

**1. INTRODUCTION**

Multi-wire cables are widely used as load-carrying members such as prestressed tendons and cables in the field of civil engineering. However, some local damage and prestress loss may occur inside of the cable during the long service life under extreme

---

<sup>1)</sup> Graduate Student

<sup>2)</sup> Professor

<sup>3)</sup> Professor

<sup>4)</sup> Professor

*The 2020 World Congress on  
The 2020 Structures Congress (Structures20)  
25-28, August, 2020, GECE, Seoul, Korea*

environment, which will affect the carrying capacity of the structure. In the past 20 years, there have been many bridge collapse accidents caused by cable failures such as Nanfangao Bridge in China, which collapsed due to the corrosion of single cable. This brought huge economic losses to the whole society. Therefore, a nondestructive testing (NDT) and structural monitoring methods are needed for damage detection to prevent serious accident.

Structural health monitoring methods have been widely used based on the global behavior of the structure to detect abnormal changes for cable-supported bridges (Cho 2010). But it cannot identify local damages such as corrosion or wire breakages on the cable. Other NDT methods like magnetic flux leakage (Li 2007), impedance method (Min 2012), and computer vision (Yao 2014) have its own limitations in accuracy, detection area, and field applications. Guided wave method is one of the most promising NDT testing methods for damage detection of a cable with the advantages of single point excitation, long distance propagation, and highly efficient detection (Kwun 1994). It works well for slender structures such as pipe, rails, and bridge cables (Zhang 2017, Wu 2018, Zhang 2018).

Guided waves can be generated by piezoelectric transducer and magnetostrictive (MS) transducer. Although the energy conversion efficiency of the piezoelectric transducer is relative higher than that of the MS transducer, the signal quality received by piezoelectric transducer is very sensitive to the coupling state between the piezoelectric sensor and the tested specimen. MS transducer has been used for cable damage detection by many researchers due to its convenience in installation and ability in actuating various modes (Laguerre 2002).

In this paper, guided wave methods are presented for the damage detection and localization on a 7-wire strand. The SAFE method was employed for analyzing the wave dispersion characteristics. The magnetostrictive transducer was used in lab-experiments for a steel strand with several cases of wire breakages and corruptions. The time of flight (TOF) information incorporate with the wave velocity were used for the damage localization. A reference-free method for damage severity estimation is proposed based on the wave energy transmission and reflection. Conclusions are drawn based on the performance of ultrasonic guided wave techniques on damage detection, localization, and quantification.

## **2. WAVE DISPERSION PROPERTY ANALYSIS**

### *2.1 Theory of the SAFE method*

The semi-analytical finite element (SAFE) analysis method is employed to calculate the wave dispersion curves for the 7-wire strand. The helical coordinate system shown in Fig. 1 is constructed by the orthonormal bases ( $N(s)$ ,  $B(s)$ ,  $T(s)$ ), where the axial coordinate  $s$  is common for all wires. Then the helical centerline can be expressed as Eq. (1) under the helical coordinates (Treyssède 2008). By this method, 3D wave propagation can be analyzed by a 2D model assuming the waves propagate along the  $s$ -direction with a harmonic exponential solution  $e^{i(k s - \omega t)}$  (where  $k$  is the wavenumber, and  $\omega$  is the frequency), which can drastically improve the computing efficiency. The displacement  $\mu(x, y, s, t)$  of guided waves can be described as Eq. (2). Using the Hamilton principle, the wave propagation equation is formulated as Eq. (3).

$$\mathbf{L}(s) = R \cos\left(\frac{2\pi}{l} s\right) \bar{x} + R \sin\left(\frac{2\pi}{l} s\right) \bar{y} + \frac{L}{l} s \bar{z} \quad (1)$$

$$\boldsymbol{\mu}(x, y, s, t) = \begin{cases} \mu_x(x, y, s, t) \\ \mu_y(x, y, s, t) \\ \mu_s(x, y, s, t) \end{cases} = \begin{cases} \mu_x(x, y) \\ \mu_y(x, y) \\ \mu_s(x, y) \end{cases} e^{i(ks - \omega t)} \quad (2)$$

$$\int_{\Omega} \delta \boldsymbol{\varepsilon}^T \boldsymbol{\sigma} \sqrt{g} dx dy ds - \omega^2 \int_{\Omega} \rho \delta \boldsymbol{\mu}^T \boldsymbol{\mu} \sqrt{g} dx dy ds = 0 \quad (3)$$

where  $R$  is the radius of the wire;  $L$  is the pitch length along the  $z$ -axis;  $l$  is the curvilinear length of each pitch ( $l = \sqrt{L^2 + 4\pi^2 R^2}$ );  $\boldsymbol{\sigma}$  and  $\boldsymbol{\varepsilon}$  denote the stress and strain vector with the stress-strain relationship  $\boldsymbol{\sigma} = \mathbf{C} \boldsymbol{\varepsilon}$ ;  $C$  is the stiffness matrix;  $\rho$  is the mass density;  $\Omega$  is the element volume;  $g = (1 + \kappa x)^2$  with the initial curvature  $\kappa = 4\pi^2 R/l^2$  of the helical wire.

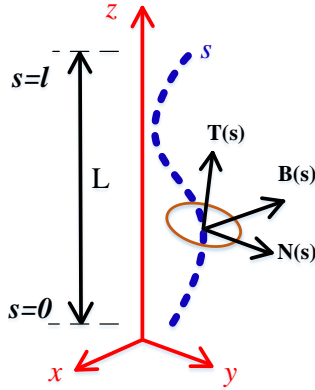


Fig. 1 The helical coordinate

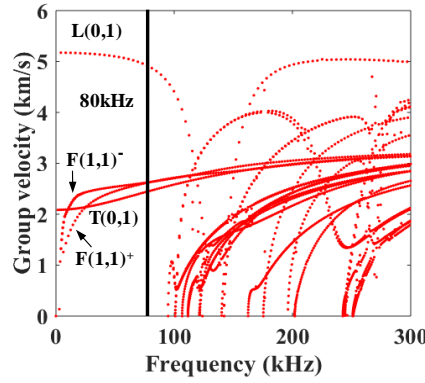


Fig. 2 Group velocity dispersion curve

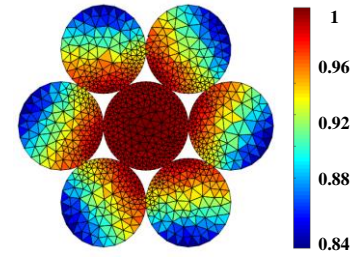


Fig. 3 Mode shape of L(0,1)

The dispersion curves of the wave modes are obtained according to the relationship between  $k$  and  $\omega$ . The phase and group velocities of each mode can be expressed as  $C_p = \omega/k$  and  $C_g = \partial\omega/\partial k$ .

## 2.2 Dispersion curve from SAFE analysis

The detailed properties of the 7-wire strand are listed in Table 1, triangular elements are used and the cross section is meshed using COMSOL, which includes 1290 points and 2266 elements. For the computation efficiency, both helical and straight wires are considered using the same coordinate; thus, the curvature and tortuosity are given by  $\kappa = 0$ , and  $\tau = 2\pi/L$ . Then, the cross section of the helical wire is perpendicular to the  $z$ -axis. The contact conditions between wires are modeled as rigid. The group velocity dispersion curve is plotted in Fig. 2, from which it can be found that the number of propagation modes increases with the exciting frequency. The excitation frequency is selected as 80kHz, at which a small number of modes exist including longitudinal (L(0,1)), flexural (F(0,1)), and torsional (T(0,1)) modes. In this study, only the first longitudinal mode is excited with the mode shape shown in Fig. 3.

Table 1. Basic properties for the steel strand.

Geometrical parameters	Outer diameter (mm)	15.2	Material properties	Young's modulus (GPa)	210
	Pitch (mm)	260		Poisson ratio	0.3
	Lay angle	7.9°		Density (kg/m <sup>3</sup> )	7850

### 3. DESIGN OF MAGNETO-STRICTIVE TRANSDUCER

#### 3.1 Configuration of permanent magnets

Ferromagnetic materials show magneto-strictive phenomena, which can be used to generate and measure the guided waves. The MS transducer consists of a permanent magnet to provide the static magnetic field and a coil unit inside to provide the dynamic magnetic field. In order to generate the longitudinal guided wave mode, both of the static magnetic and the dynamic magnetic fields shall be parallel to the longitudinal direction of the test specimen. Meanwhile, the magnetic field shall be uniformly distributed on the whole cross section to avoid the generation of non-axisymmetric modes. Furthermore, to generate a guided wave with higher energy conversion efficiency, the magnetic induction intensity of the permanent magnet shall be controlled.

The total length of the MS transducer is designed to be 70 mm. Fig. 4 shows the configuration of the magnet unit which consists of three pairs of NdFeB N35 permanent magnets with the size 15×6×4 mm. Three saddle blocks are adopted to connect the magnets to form an integrated magnet loop with dimensions 70×6×5 mm.

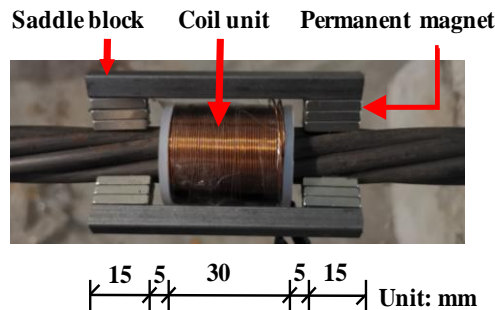


Fig. 4 Configuration of the MS transducer

#### 3.2 Configuration of the coil unit

The coil unit works as the signal actuator and receiver. As a signal actuator, it provides the bi-directional dynamic magnetic field by feeding an alternating current. Meanwhile, the changed of the magnetic induction intensity inside of the coil unit caused by the stress will be measured by voltage output. To facilitate the installation of the MS transducer on different locations of the cable, the coil was wound around a hollow plastic cylinder, whose inner diameter was slightly larger than the 7-wire strand. In this case, 200 turns were used with the total length that is half of the wavelength of the excitation signal. The group wave velocity of the L(0,1) mode at the excitation frequency of 80 kHz was 4850 m/s from the dispersion curve, thus, the length of the coil was taken as 30 mm.

#### 4. WIRE BREAKAGE DETECTION

##### 4.1 Damage localization

Experiments were carried out using the designed magneto-strictive transducer. Artificial wire breakages with the length of 1.5 mm are inflicted at 3 locations on the 7-wire strand. Fig. 5 depicts the layout of the transducers and the positions of damage, whereas Fig. 6 shows signals received at the transducer. Wave Packets 1-2 are related to the excitation and Wave Packets 3-8 are the reflected signals from 3 defects, while Wave Packets 9-10 are those reflected from the right end.

Firstly, the averaged wave velocity was determined as 4930 m/s from the undamaged signal, while the theoretical value from the SAFE analysis is 4850 m/s. Then, the acoustical distances were calculated for each wave packet using the time of flight (ToF) information and the wave velocity from the experiment. The damage localization results match very well to the real damage locations with errors less than 2%.

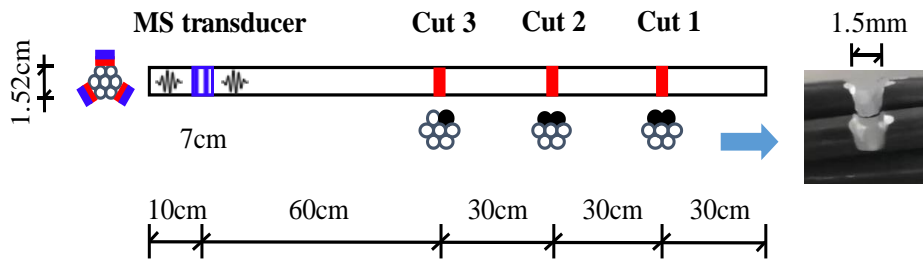


Fig. 5 Layout of the magneto-strictive transducer and 3 artificial wire breakages

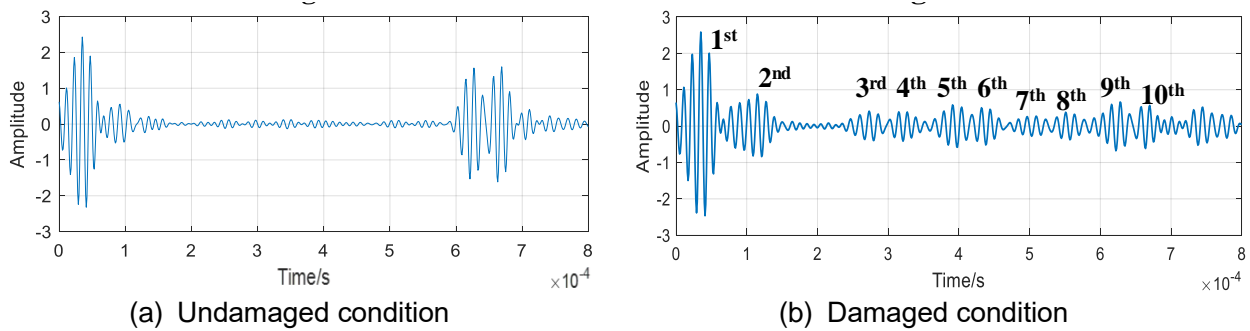


Fig. 6 Received signals from the transducer

##### 4.2 Damage severity estimation

In order to find the relationship between the received signal and the damage severity, numerical simulation and experimental studies were conducted on the same cable with increasing numbers of broken wires at three locations. It can be observed that the amplitudes of the wave packets reflected from the damage increased as the number of broken wires increased. Then, the continuous wavelet transform was carried out using “Morlet” wavelet on the wave packets to determine the wave energy of each wave packet. A reference-free method is proposed to estimate the damage severities based on the wave energy transmission coefficients ( $\alpha_i$ ) at damage locations. The wave energy transmission coefficient is defined as the ratio of the transmitted energy to the

*The 2020 World Congress on  
The 2020 Structures Congress (Structures20)  
25-28, August, 2020, GECE, Seoul, Korea*

total incoming energy at a damage location, which is related to the area reduction ratio on the multiple cable damages. It has been found that the wave energy transmission coefficients calculated for multiple damages from both numerical simulation and experimental results are in great agreement with the area remaining ratios of the steel cable with error less than 6% as shown in Table. 2, which can be used to estimate the damage severity.

**Table 2 Wave energy transmission coefficients and area remaining ratios**

Damage Cases		Wave Energy Transmission coefficients			FE Simulation Difference** (%)	Area Remaining Ratios Error*** (%)	Damage in Previous Test
Cut	Case*	$\alpha_1$	$\alpha_2$	$\alpha_3$			
Cut1	1a	0.945	-	-	0.921 (2.4)	0.929 (1.6)	No
	1b	0.831	-	-	0.853 (2.2)	0.857 (2.6)	
	1c	0.793	-	-	0.806 (1.3)	0.786 (0.7)	
	1d	0.716	-	-	0.738 (2.2)	0.714 (0.2)	
Cuts 1 & 2	2a	0.694	0.907	-	0.934 (2.7)	0.929 (2.2)	Cut 1 with Breakage (1d)
	2b	0.736	0.811	-	0.866 (5.5)	0.857 (4.6)	
	2c	0.735	0.781	-	0.832 (5.1)	0.786 (0.5)	
	2d	0.685	0.748	-	0.760 (1.2)	0.714 (3.4)	
Cuts 1, 2, & 3	3a	0.702	0.739	0.938	0.937 (0.1)	0.929 (0.9)	Cuts 1 & 2 with Breakage (1d & 2d)
	3b	0.708	0.745	0.861	0.878 (1.7)	0.857 (0.4)	
	3c	0.686	0.726	0.792	0.830 (3.8)	0.786 (0.6)	
	3d	0.680	0.751	0.740	0.743 (0.3)	0.714 (2.6)	

Notes:

\*Numbers of wire breakage increase as 0.5, 1, 1.5, and 2 for a, b, c, and d, respectively.

\*\*Differences in parentheses are between the experiment and FE simulation results for  $\alpha_i$ .

\*\*\*Errors in parentheses are the estimated  $\alpha_i$  vs the area remaining ratios.

## 5. CORROSION DETECTION

### 5.1 Corrosion simulation

Corrosion was artificially inflicted on the cable using the accelerated electrochemical method as shown in Fig. 7, which can induce significant corrosion in a short time. The material and geometrical properties of the cable were the same with the previous values. Direct current of 0.5 A was applied to the 7-wire strand using a potentiometer. Two segments of the steel strand were immersed into 5% sodium chloride (NaCl) electrolyte solution. Current direction was controlled to make the steel stand served as the anode and a small copper plate immersed into the electrolyte solution worked as a cathode. Experiment was carried out on the cable with various corrosion severities for 6 days.

### 5.2 Corrosion localization and severity estimation

Corrosion localization was carried out using the average ToF information obtained from the peak values of Hilbert envelopes and average wave velocity (4930 m/s), which is well agreed with real locations with an error less than 4%. The wave energy

transmission coefficients were calculated by treating each corrosion segment as a defect. It shows good agreement with the area remaining ratios of the cross section within 6% error as in Fig. 8.

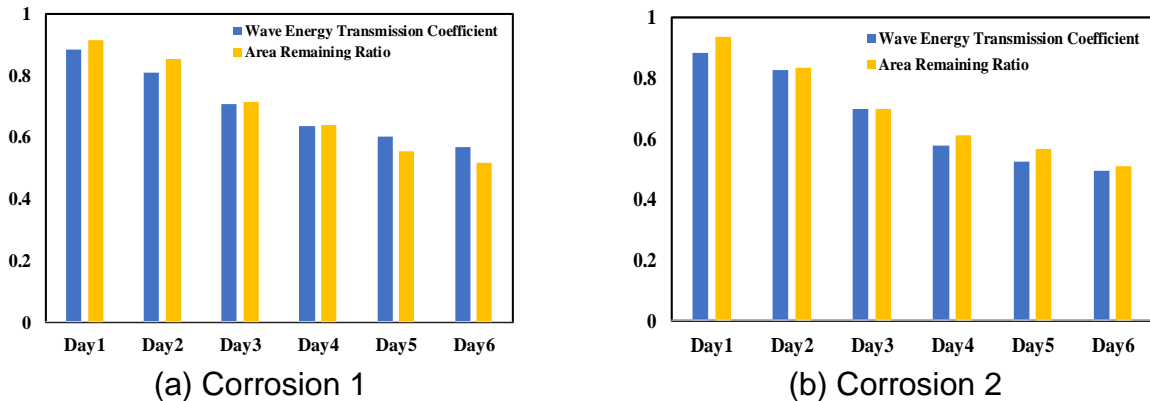
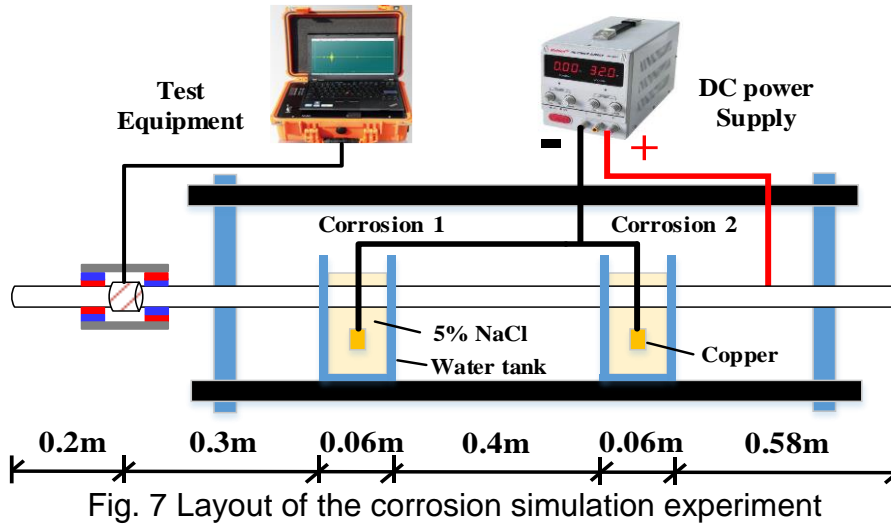


Fig. 8 Wave energy transmission coefficients of the two corroded segments

## 6. CONCLUSION

In this study, a guided wave method is presented for damage detection in a 7-wire strand using magneto-strictive transducers. The SAFE-based wave dispersion analysis for the helical wire cable provide a good reference for choosing an excitation frequency and mode shape. The wave velocity obtained from the dispersion curve matches reasonably well to the experiment result. Wire breakages and corrosions are artificially inflicted at various locations with different severity. Damage locations are successfully estimated using the time of flight information and wave velocity with errors less than 2%. Damage severities were estimated using the proposed reference-free method based on the wave transmission coefficients, which showed excellent agreement with the area remaining ratios of the cross section at the damage locations with errors less than 6%.

*The 2020 World Congress on  
The 2020 Structures Congress (Structures20)  
25-28, August, 2020, GECE, Seoul, Korea*

## **ACKNOWLEDGMENTS**

The authors acknowledge the supports from the National Key R&D Program of China (2018YFE0125400, 2017YFC0806100) and National Science Foundation of China (U1709216).

## **REFERENCES**

- Cho, S., Jo, H., Jang, S., Park, J., Jung, H.J., & Yun, C.B., et al. (2010). Structural health monitoring of a cable-stayed bridge using smart sensor technology: deployment and evaluation. *Smart Structures & Systems*, 6(5-6), 439-459.
- Kwun, H. (1994). Magnetostrictive generation and detection of longitudinal, torsional, and flexural waves in a steel rod. *Journal of the Acoustical Society of America*, 96(6), 500-507.
- Laguerre, L., Aime, J.C., Brissaud, M. (2002). Magnetostrictive pulse-echo device for non-destructive evaluation of cylindrical steel materials using longitudinal guided waves. *Ultrasonics*, 39(7), 503-514.
- Li, Y., Wilson, J., Tian, G.Y. (2007). Experiment and simulation study of 3D magnetic field sensing for magnetic flux leakage defect characterization. *NDT & E international*, 40(2):179-184.
- Min, J.Y., Shim, H.J, Yun, C.B., Hong, J.W. (2016). An electromechanical impedance-based method for tensile force estimation and damage diagnosis of post-tensioning systems. *Smart Structures and Systems*, 17(1):107-122.
- Treysède, F. (2008). Elastic waves in helical waveguides. *Wave Motion*, 45(4), 457-470.
- Wu, J.J., Tang, Z.F., Lv, F.Z., Yang, K.J., Yun, C.B., Duan, Y.F. (2018). Ultrasonic guided wave-based switch rail monitoring using independent component analysis, *Measurement Science and Technology*, 29, 115102.
- Yao, Y., Tung, S.T.E., Glisic, B. (2014). Crack detection and characterization techniques-an overview. *Structural Control and Health Monitoring*, 21(12), 1387-1413.
- Zhang, X.W, Tang, Z.F, Lv, F.Z, Yang, K.J. (2017). Scattering of torsional flexural guided waves from circular holes and crack-like defects in hollow cylinders. *NDT & E international*, 89(JUL.), 56-66.
- Zhang, P.F., Tang, Z.F., Duan, Y.F., Yun, C.B., Lv, F.Z. (2018). Ultrasonic guided wave approach incorporating SAFE for detecting wire breakage in bridge cable. *Smart Structures and Systems*, 22(4):481-493.